Small Molecule Chemisorption on Indium−Tin Oxide Surfaces: Enhancing Probe Molecule Electron-Transfer Rates and the Performance of Organic Light-Emitting Diodes†

Chet Carter,‡ Michael Brumbach,‡ Carrie Donley,‡,⊥ Richard D. Hreha,‡ Seth R. Marder,§ Benoit Domercq,|| SeungHyup Yoo,|| Bernard Kippelen,|| and Neal R. Armstrong*,‡

Department of Chemistry, University of Arizona, Tucson, Arizona 85721, and Schools of Chemistry and Biochemistry and Electrical and Computer Engineering, Georgia Institute of Technology, Atlanta, Georgia 30332

Received: June 28, 2006; In Final Form: September 3, 2006

Indium−tin oxide (ITO) surfaces have been modified by chemisorption of carboxylic acid functionalized small molecules: ferrocene dicarboxylic acid (**1**), 3-thiophene acetic acid (**2**), and 6-{4-[{4′-[[4-(5-carboxy-pentyloxy)-phenyl]-(4-methoxy-phenyl)-amino]-biphenyl-4-yl}-(4-methoxy-phenyl)-amino]-phenoxy}-hexanoic acid (p-OMe)$_2$-TPD-(C_5-COOH)$_2$) (**3**). Voltammetrically determined surface coverages of **1**−**3** increased in two stages, the first stage completing in minutes, the latter stage taking several hours. Electron-transfer rate coefficients, k_S, for the probe molecule ferrocene in acetonitrile likewise increased in two stages with increasing surface coverages of **1**, **2**, and **3**. Fourier transform infrared spectroscopy of In_2O_3 powders, exposed for long periods to ethanol solutions of each modifier, confirmed the formation of indium oxalate-like surface species. X-ray photoelectron spectroscopy of carboxy-terminated alkanethiol-modified gold surfaces, exposed to these same In_2O_3(powder)/small molecule modifier solutions, showed the capture of trace levels of indium as a result of the chemisorption of these small molecules, suggesting that slow etching of the ITO surface also occurs during the chemisorption event. Conventional aluminum quinolate/bis-triarylamine organic light-emitting diodes (OLEDs) created on ITO surfaces modified with **1**, **2**, and **3**, with and without an overlayer of PEDOT:PSS (a poly(thiophene)/poly(stryenesulfonate) ITO modifier), showed leakage currents lowered by several orders of magnitude and an increase in OLED device efficiency.

Introduction

Transparent conducting oxide (TCO) thin films are widely used in an expanding variety of organic light-emitting diode (OLED) displays and organic photovoltaic (OPV) technologies.[1−34] Indium−tin oxide (ITO) has the attractive combination of high optical transparency and good electrical conductivity; however, these TCO films often have a root-mean-square (rms) surface roughness in excess of 3 nm, their surface energies are not well matched to nonpolar organic films, and they can show extremely variable electrical properties over a single device of area less than 0.1 cm^2.[35−38] Several cleaning and modification procedures have been described for ITO surfaces.[5−21,28−34,36−46] These pretreatments have generally been designed to enhance the effective work function of the TCO thin film, its wettability by organic layers, and its stability in device operation. One of the most widely used modification strategies involves electrodeposition or spin-casting of a thin layer of a conductive polymer (CP) prior to deposition of the electroluminescent small molecules or polymers.[42−46] The most common of these CP layers is PEDOT:PSS, a polyelectrolyte consisting of oligomers of poly(3,4-diethoxythiophene) and higher molecular weight poly(styrenesulfonate), which planarizes the TCO surface and enhances its interaction with organic thin films. Its ionic composition, however, can be difficult to control, and the sulfonic acid substituents in PEDOT:PSS can present an acidic microenvironment to the ITO/CP interface.[45,46] Modification with CP layers, especially PEDOT:PSS, does provide for an effective means of enhancing the apparent work function of the bottom contact in OLED and OPV technologies.[19,45]

The surface composition of commercially available ITO thin films is complex, consisting of a mixture of the stoichiometric oxide (In_2O_3), an oxy-hydroxide-like species (InOOH), and a significant coverage of monomeric and oligomeric In(OH)$_3$-like species, resulting from the hydrolysis of the ITO surface immediately after sputter deposition, upon exposure to even trace levels of water vapor, in addition to carbonaceous contaminants.[11−15] The role played by tin dopants and their distribution in the near-surface region may also be in question. In some instances they provide a convenient site for specific modification chemistries on the ITO surface; however some studies suggest that these dopants may not be distributed uniformly and that the stoichiometry and crystallinity of these species are quite variable.[1,28−31,46]

Several researchers have shown that small molecules such as ferrocene dicarboxylic acid (Fc(COOH)$_2$) (**1** in Figure 1) chemisorb to the ITO surface from polar solvents such as ethanol.[36,37,41,47−50] Carboxylic acid functionalities are thought to adsorb to oxide surfaces through weak electrostatic and hydrogen-bonding interactions and for some oxides coordinate−covalent bonding between the carboxylate and the metal ion defect sites. Both the surface coverage (determined voltammetrically in a less polar solvent like acetonitrile) and the rate

† Part of the special issue "Arthur J. Nozik Festschrift".

* Author to whom correspondence should be addressed. E-mail: nra@u.arizona.edu.

‡ Department of Chemistry, University of Arizona.

§ School of Chemistry and Biochemistry, Georgia Institute of Technology.

|| School of Electrical and Computer Engineering, Georgia Institute of Technology.

⊥ Current Address: Hewlett-Packard, Palo Alto, CA 94304.

10.1021/jp064061g CCC: $33.50
Published on Web 11/03/2006

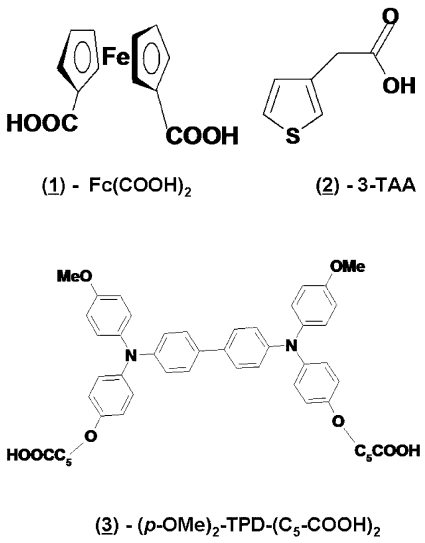

Figure 1. Schematic views of the small molecule surface modifiers used in this study.

of oxidation/reduction of adsorbed $Fc(COOH)_2$ are sensitive to the pretreatment and cleaning procedures used to prepare the ITO electrode.

We now demonstrate the extension of this approach to chemisorb **1** and two other small molecule modifiers to the ITO surface: 3-thiophene acetic acid (3-TAA) (**2**) and a modified version of the hole transport agent, TPD (4,4′-bis(*m*-tolylphenlyamino)biphenyl)—with two *para*-methoxy substituents and two six-carbon alkoxy side chains, terminated in carboxylic acids (6-{4-[{4′-[[4-(5-carboxy-pentyloxy)-phenyl]-(4-methoxyphenyl)-amino]-biphenyl-4-yl}-(4-methoxy-phenyl)-amino]-phenoxy}-hexanoic acid (p-OMe)$_2$-TPD-(C_5-COOH)$_2$) (**3**). Schematic views of these molecules are seen in Figure 1.

Adsorbed **1** has been used previously to determine the fraction of electrochemically active sites on ITO surfaces that had been treated by a variety of plasma cleaning and chemical etchant activation procedures.[36] Compound **1** has also been shown to mediate the electron transfer of solution probe molecules, such as Fc/Fc^+, in less polar solvents such as acetonitrile. Compound **2** is a readily available thiophene derivative that chemisorbs to ITO surfaces and is under evaluation as a "nucleation site" for electropolymerized thiophene polymers grown on the ITO surface.[51] The oxidation potential for 3-TAA is positive of the $E°$ for Fc/Fc^+ (ca. 1.0 V) and is therefore not expected to mediate electron transfer to Fc/Fc^+. Compound **3** was selected to provide a chemisorbed surface species more easily oxidized than both Fc and TPD and to mediate the redox chemistry of solution probes such Fc/Fc^+ and hole injection into condensed phase TPD layers in OLEDs.[52]

Using previous studies of small molecule chemisorption as a guide,[29−32,36,37,41,49,50] each of these small molecules was chemisorbed to ITO surfaces at concentrations and exposure times designed to ensure monolayer coverage. Water contact angles confirmed a decrease in polarity of the ITO surface after modification. We also observed enhancements in electron-transfer rates (k_S) of the oxidation/reduction of the probe molecules Fc/Fc^+ and TPD/TPD^+ in acetonitrile. At low sweep rates the voltammetric oxidation of Fc showed evidence of an electrocatalytic effect for ITO surfaces modified with **1** and **3**. Simple two-layer OLED devices (ITO/TPD/Alq_3/Mg:Ag)[53] were fabricated on comparable modified ITO substrates, and significant increases in OLED efficiency (and decreases in leakage currents) were noted with modification with each of the small molecules. Enhancements were also noted even when PEDOT:PSS layers were spin-cast over the small molecule modified ITO surface.

Experimental Section

Chemicals received from commercial sources were used without further purification. Compounds **1**, $Fc(COOH)_2$, and **2**, 3-TAA, were obtained from Aldrich, and used as received. Lithium percholorate was used as the supporting electrolyte in all electrochemical experiments. All NMR spectra were recorded with a Varian Unity Plus spectrometer at 300 MHz (^{1}H) and 75 MHz (^{13}C) in $CDCl_3$ or $(CD_3)_2CO$ unless otherwise stated. Spectra were internally referenced relative to tetramethylsilane (TMS; $\delta(^1H) = 0$ ppm; $\delta(^{13}C) = 0$ ppm) using either the TMS ^{1}H resonance or the ^{13}C resonance of the solvent. UV−vis spectra were recorded in thin films on quartz substrates with a Hewlett-Packard 8453 spectrometer. Gas chromatography/mass spectrometry (GC/MS) was performed on a Hewlett-Packard HP6890 GC with a Hewlett-Packard 5973 mass spectrometer.

Synthesis of 3. *(4-Bromophenoxy)(tert-butyl)dimethylsilane.* To a 500 mL round-bottom flask equipped with a magnetic stir bar and containing an argon atmosphere were added 4-bromophenol (15.0 g, 86.7 mmol), *tert*-butyldimethylsilyl chloride (15.7 g, 104 mmol), and 40 mL of dimethylformamide. Imidazole (7.1 g, 104 mmol) was added, and the mixture was stirred. The reaction was followed by thin-layer chromatography (TLC). Upon the disappearance of 4-bromophenol the reaction mixture was poured into a separatory funnel containing 50 mL of ice-cold water and 100 mL of diethyl ether. The ether layer was collected and washed with 5 × 50 mL portions of ice-cold water. The solvent was removed under reduced pressure, and the product was purified by flash chromatography over silica gel eluting with hexanes. The fractions were combined, and the solvent was removed under reduced pressure. The residual solvent was removed in vacuo. The yield of the desired product isolated as a colorless oil was 23.82 g (95.6%). ^{1}H NMR (500 MHz, $CDCl_3$): δ 0.19 (s, 6 H), 0.98 (s, 9 H), 6.73 (d, $J = 9.0$ Hz, 2 H), 7.33 (d, $J = 9.0$ Hz, 2 H). ^{13}C NMR (125 MHz, $CDCl_3$): δ −4.52, 18.16, 25.60, 113.57, 121.88, 132.24, 154.79.

N,N′-Bis(4-{[tert-butyl(dimethyl)silyl]oxy}phenyl-N,N′-bis(4-methoxyphenyl)-1,1′biphenyl-4,4′-diamine. To a 500 mL round-bottom flask equipped with a magnetic stir bar and filled with argon was added 100 mL of toluene. The toluene was deoxygenated by bubbling argon through the solvent for 10 min. *N,N′*-Bis(4-methoxyphenyl)-1,1′-biphenyl-4,4′diamine (6.0 g, 15.13 mmol) was dissolved. (4-Bromophenoxy)(*tert*-butyl)dimethylsilane (9.57 g, 33.3 mmol), $Pd_2(dba)_3$ (0.46 g, 0.50 mmol), and diphenylphosphino ferrocene (0.55 g, 1.0 mmol) were added. After the solution was mixed for 10 min sodium *tert*-butoxide (3.8 g, 39.9 mmol) was added. The reaction mixture was stirred while being followed by TLC. Upon the disappearance of the starting material the reaction was filtered through a plug of silica gel eluting with dichloromethane. The product was purified by flash chromatography over silica gel eluting with 1:1 dichloromethane/hexanes. The proper fractions were combined, and the solvent was removed under reduced pressure. The residual solvent was removed in vacuo, and 7.25 g (8.96 mmol) of the product was isolated as a pale brown solid (59.2%). ^{1}H NMR (500 MHz, $CDCl_3$): δ 0.22 (s, 12 H), 1.01 (s, 18 H), 3.81 (s, 6 H), 6.76 (d, $J = 9.0$ Hz, 4 H), 6.85 (d, $J = 9.0$ Hz, 4 H), 6.99 (m, 8 H), 7.09 (d, $J = 8.0$ Hz, 4 H), 7.38 (d, $J = 8.5$ Hz, 4 H). ^{13}C NMR (125 MHz, ($CDCl_3$): δ −4.42, 18.15, 25.67, 55.44, 114.58, 114.71, 120.59, 121.16, 122.91, 126.04, 126.44, 126.82, 133.00, 141.02, 141.43, 147.35, 151.41, 155.65. Anal. Calcd

for $C_{50}H_{60}N_2O_4Si_2$: C, 74.21; H, 7.47; N, 3.46. Found: C, 74.45; H, 7.59; N, 3.49. HRMS Calcd for $C_{50}H_{60}N_2O_4Si_2$: 808.4092. Found 808.4085.

4-[{4′-[(4-Hydroxyphenyl)(4-methoxyphenyl)amino]-1,1′-biphenyl-4-yl}(4-methoxyphenyl)amino]phenol. To a 250 mL round-bottom flask equipped with a magnetic stir bar were added *N*,*N*′-bis(4-{[*tert*-butyl(dimethyl)silyl]oxy}phenyl-*N*,*N*′-bis(4-methoxyphenyl)-1,1′-biphenyl-4,4′-diamine (7.25 g, 8.95 mmol) and 50 mL of tetrahydrofuran (THF). The *N*,*N*′-bis(4-{[*tert*-butyl(dimethyl)silyl]oxy}phenyl-*N*,*N*′-bis(4-methoxyphenyl)-1,1′-biphenyl-4,4′-diamine was dissolved, and 25 mL of 1.0 M tetrabutylammonium fluoride (0.25 mmol) in THF was added. The solution was mixed while the progress of the reaction was followed by TLC. Upon the disappearance of *N*,*N*′-bis(4-{[*tert*-butyl(dimethyl)silyl]oxy}phenyl-*N*,*N*′-bis(4-methoxyphenyl)-1,1′-biphenyl-4,4′-diamine the reaction mixture was poured into a separatory funnel containing 100 mL of water and 100 mL of diethyl ether. The water layer was extracted with 3 × 50 mL portions of diethyl ether. The ether layers were combined, and the solvent was removed under reduced pressure. The product is purified by flash chromatography over silica gel eluting with dichloromethane. The proper fractions were combined, and the solvent was removed under reduced pressure. The residual solvent was removed in vacuo. The yield of the product isolated as a pale brown glassy solid was 4.40 g (84.7%). ^{1}H NMR (500 MHz, $(CD_3)_2CO$): δ 3.77 (s, 6 H), 6.83 (d, J = 9.5 Hz, 4 H), 6.87 (d, J = 4.5 Hz, 4 H), 6.89 (d, J = 4.5 Hz, 4 H), 6.97 (d, J = 9.0 Hz, 4 H), 7.04 (d, J = 8.5 Hz, 4 H), 7.40 (d, J = 9.0 Hz, 4 H), 8.45 (s, 2 H). ^{13}C NMR (125 MHz, $(CD_3)_2CO$): δ 54.78, 114.60,116.13, 120.14, 126.27, 126.51, 127.10, 132.30, 139.64, 140.94, 147.74, 154.04, 155.92. Anal. Calcd for $C_{39}H_{32}N_2O_4$: C, 78.60; H, 5.55; N, 4.82. Found: C, 78.29; H, 5.62; N, 4.70. HRMS Calcd for $C_{39}H_{32}N_2O_4$: 580.2362. Found: 580.2357.

6-{4-[{4′-[[4-(5-Ethoxycarbonyl-pentyloxy)-phenyl]-(4-methoxy-phenyl)-amino]-biphenyl-4-yl}-(4-methoxy-phenyl)-amino]-phenoxy}-hexanoic Acid Ethyl Ester. To a 500 mL round-bottom flask were added 4-[{4′-[(4-hydroxyphenyl)(4-methoxyphenyl)-amino]-1,1′-biphenyl-4-yl}(4-methoxyphenyl)amino]phenol (4.60 g, 7.42 mmol), ethyl 6-bromohexanoate (3.57 g, 16.0 mmol), acetone (50 mL), and potassium carbonate (19.35 g, 140 mmol). The reaction was stirred at room temperature while being followed by TLC. Upon the disappearance of 4-[{4′-[(4-hydroxyphenyl)(4-methoxyphenyl)amino]-1,1′-biphenyl-4-yl}-(4-methoxyphenyl)amino]phenol the mixture was poured into a separatory funnel containing 100 mL of water. The product was extracted in diethyl ether. The solvent was removed under reduced pressure. The material was purified by flash chromatography over silica gel eluting with 1:49 ethyl acetate/dichloromethane. The solvent was removed under reduced pressure, and the residual solvent was removed in vacuo. The yield of the desired product, isolated, as a pale yellow glass, was 6.18 g (90.2%). ^{1}H NMR (500 MHz, $CDCl_3$): δ 1.21 (t, J = 6.5 Hz, 6 H), 1.51 (quint, J = 5.5 Hz, 4 H), 1.68 (quint, J = 8.0 Hz, 4 H), 1.79 (quint, J = 6.5 Hz, 4 H), 2.33 (t, J = 8.0 Hz, 4 H), 3.79 (s, 6 H), 3.98 (t, J = 6.5 Hz, 4 H), 4.08 (quart., J = 7.5 Hz, 4 H), 6.90 (m, 12 H), 7.04 (dd, J = 2.5 Hz, 6.5 Hz, 8 H), 7.43 (d, J = 8.5 Hz, 4 H). ^{13}C NMR (125 MHz, $CDCl_3$): δ 13.67, 24.52, 25.41, 33.64, 54.80, 59.58, 67.64, 114.64, 115.24, 120.57, 126.45, 126.58, 132.54, 140.70, 140.80, 147.58, 155.53, 156.05, 172.71. Anal. Calcd for $C_{54}H_{60}N_2O_8$: C, 74.97; H, 6.99; N, 3.24. Found: C, 74.77; H, 7.11; N, 3.32.

6-{4-[{4′-[[4-(5-Carboxy-pentyloxy)-phenyl]-(4-methoxy-phenyl)-amino]-biphenyl-4-yl}-(4-methoxy-phenyl)-amino]-phenoxy}-hexanoic Acid (3). To a 500 mL round-bottom flask were added 4-[{4′-[(4-methoxyphenyl){(4-[6-oxooctyl)oxy]phenyl}-amino]-1,1′-biphenyl-4-yl]amino}phenoxy)octan-3-one (6.08 g, 7.03 mmol), THF (10 mL), potassium hydroxide (2.0 mL, 18 M) and a magnetic stir bar. The reaction was refluxed while being followed by TLC. A white precipitate develops as the reaction proceeds. Upon the disappearance of 4-[{4′-[(4--methoxyphenyl){(4-[6-oxooctyl)oxy]phenyl}amino]-1,1′-biphenyl-4-yl]amino}phenoxy)octan-3-one the white solid was collected by vacuum filtration. The solid was rinsed three times with 10 mL portions of THF and then transferred to a 1000 mL beaker containing a stir bar and 500 mL of water. The solution was stirred, and 10 mL of 1 M HCl was added over 10 min. The mixture was then extracted with 5 × 100 mL portions of diethyl ether. The solvent was removed under reduced pressure, and the residual solvent was removed in vacuo while intermittently heating above the melting temperature. The yield of the desired product, isolated, as a pale yellow glass was 3.79 g (66.7%). ^{1}H NMR (500 MHz, $(CD_3)_2CO$): δ 1.51 (quint, J = 5.5 Hz, 4 H), 1.67 (quint, J = 8.0 Hz, 4 H), 1.76 (quint, J = 6.5 Hz, 4 H), 2.06 (quint, J = 1.5 Hz), 2.32 (t, J = 8.0 Hz, 4 H), 3.78 (s, 6 H), 3.98 (t, J = 6.5 Hz, 4 H), 6.90 (m, 12 H), 7.01 (dd, J = 2.5 Hz, 6.5 Hz, 8 H), 7.37 (d, J = 8.5 Hz, 4 H). ^{13}C NMR (125 MHz, $(CD_3)_2CO$): δ 24.55, 25.50, 33.37, 54.80, 59.82, 67.70, 114.65, 115.24, 120.65, 126.26, 126.42, 132.51, 140.68, 140.80, 147.54, 155.51, 155.99, 174.11. Anal. Calcd for $C_{50}H_{52}N_2O_8$: C, 74.24; H, 6.48; N, 3.46. Found: C, 74.32; H, 6.26; N, 3.47. HRMS Calcd for $C_{50}H_{52}N_2O_8$: 808.3724. Found: 808.3726.

ITO Cleaning. ITO-coated glass (nominal Sn/In atomic ratio of 1:10) was obtained commercially (Colorado Concept Coatings LLC, Longmont, CO) and cut to the appropriate device size prior to cleaning. Samples for a particular set of devices or electrochemical experiments were selected to be adjacent to each other on the larger sheet of ITO to minimize variations in the device and electrochemical properties that arise due to small variations in ITO processing. Prior to being cleaned, ITO samples for electrochemical experiments were masked off and etched with 15% HCl solution heated to 80 °C to create a 2 × 10 mm^2 band electrode (0.2 cm^2), with external contact pads.[51] Similarly, ITO samples for OLED devices were masked and coated in select regions with an insulating layer of SiO to create a device area of ca. 0.2 cm^2.

Each ITO sample was then taken through a series of cleaning steps: (i) Samples were first rubbed with a soft cotton cloth saturated with soapy water and thoroughly rinsed with filtered water (Millipore filtering system, 18 MΩ); (ii) samples were cleaned in an ultrasonic bath (30 min each cycle) in filtered water/Triton X-100, filtered water and finally pure ethanol; (iii) samples then were dried in a stream of nitrogen and etched in an air-plasma cleaner (Harrick, 60 W) for 5 min just prior to surface modification and/or device preparation.

ITO Modification. For small molecule chemisorption, freshly cleaned ITO samples were immersed in 10 mM solutions of the small molecule, in ethanol, and left for periods of up to 8 h. After chemisorption, the samples were emmersed and rinsed thoroughly with acetonitrile (Aldrich) and dried in a stream of nitrogen. Some samples were modified by spin-coating a layer of PEDOT:PSS (Baytron P-EC grade, H. C. Stark Company). The ITO sample was mounted on an Integrated Technologies Inc. spin-coater, fully covered by the PEDOT:PSS/alcohol/water solution (ca. 0.5 mL), and spun at 3000 rpm for 60 s to dryness. The newly formed film was then annealed in a vacuum oven at 100 °C for 1 h and the cooled to room temperature before use.

This type of modification was applied to freshly cleaned ITO as well as ITO samples with chemisorbed small molecules.

Determination of Water Contact Angles. Water contact angles were made on at least 10 separate droplets per ITO sample, utilizing a Kruss DSA 1.7 drop shape analysis instrument that allows for automated delivery and calibrated volumes (50 μL) to maximize reproducibility. ITO samples were prepared according to the steps above for modified and nonmodified surfaces and placed on the mobile sample stage where a series of small droplets of filtered water were deposited laterally across the sample surface. The contact angle was then quickly measured for each droplet, on both sides of the drop, with only a few elapsed seconds after drop delivery, to avoid significant interaction between the chemisorbed small molecules and the water droplet.

Atomic Force Microscopy Studies. Surface images of as-received, cleaned/unmodified, and modified ITO samples were taken with a Nanoscope III atomic force microscope operating in tapping mode. Images were taken in a minimum of four placements across the sample to ensure representative images.

X-ray Photoelectron/UV Photoelectron Spectroscopy. X-ray photoelectron spectroscopy (XPS)/ultraviolet photoelectron spectroscopy (UPS) studies were conducted with a Kratos Axis-Ultra X-ray photoelectron spectrometer with a monochromatic Al Kα source (1486.6 eV) and a He(I) (21.2 eV) source (Omicron). Spectra were taken with a high take-off angle (75°) to maximize surface sensitivity.[34] ITO samples were either analyzed as-cleaned and modified or were occasionally sputter-cleaned with an argon-ion sputter gun (45 min, 0.75 keV).

XPS of self-assembled monolayer (SAM)-covered gold was carried out by exposing 3.0 g of In_2O_3 powder (ca. 150 m^2 per gram) to ITO modification solutions similar to those used for ITO (0.01 M). In_2O_3 powders have been shown to be similar in composition to ITO but provide high surface areas to maximize the $In(OH)_x$ material that may potentially be lost to solution. After a sufficient elapsed time to achieve equilibrium had passed, (approximately 8 h) the solution was collected, double-filtered, and exposed to gold samples that had been modified previously with an alkanethiol carboxylic acid ($SH(CH_2)_{12}$-COOH). The carboxylic acid functionalized SAM was utilized to complex with and preconcentrate any indium or indium carboxylate-like complex present in the modification solution. The gold samples were allowed to soak overnight in the collected modification solutions before rinsing with ethanol and placing under vacuum.

Voltammetric Characterization of Probe Molecules. Cyclic voltammetry of cleaned and modified ITO surfaces was conducted in acetonitrile solutions using a custom three-port electrochemical cell incorporating a Ag/AgCl pseudo-reference electrode and platinum counter electrode, with an EG&G model 283 potentiostat/galvanostat. Test solutions consisted of either (i) just 0.25 M $LiClO_4$ in freshly distilled acetonitrile, for experiments where just the electrochemical activity of the chemisorbed molecules was of interest, (ii) 1 mM ferrocene (Fc), or (iii) 1 mM TPD.

OLED Device Preparation and Testing. After the cleaning and/or modification steps select ITO samples were placed in a custom-designed high vacuum deposition chamber, base pressure ca. 10^{-8} Torr (Kurt J. Lesker Corp.). Successive layers of TPD and aluminum quinolate (Alq_3) were vacuum-deposited through a mask to a thickness of 50 nm for each layer. The two-layer device was then coated with a cathode layer consisting of a codeposit of 10:1 Mg/Ag (100 nm). OLED devices were transferred to a Vacuum Atmospheres glovebox (less than 1 ppm O_2, H_2O) without exposure to atmosphere. Both current−voltage and luminance−voltage measurements were made with a Keithly 2400 Source Meter and a calibrated photodiode positioned perpendicular to the device face (calibrated to provide correct luminance measurements across the full visible wavelength region).

Results and Discussion

ITO Surface Composition. Figure 2 summarizes the state of the ITO surface as discussed in recent publications from this group and others and the proposed modes of chemisorption of small molecules such as **1**.[1,11−15,25,26,36−38] Typical commercially available ITO thin films sputter-deposited to a thickness of ca. 100−200 nm consist of crystalline grains, which vary from 0.05 to 0.2 μm in diameter, consisting predominantly of either the ⟨111⟩ or ⟨100⟩ faces of the bixebyte unit cell, with the rms roughness ranging from ca. 0.8 to 3.0 nm.[36−38] The high electrical conductivity in ITO arises from two types of dopant sites: (i) oxygen lattice vacancy sites (V_O:s^2) or (ii) Sn^{3+} or Sn^{2+} species in interstitial sites normally occupied by indium.[1,54] Recent XPS/UPS studies in our group of clean, freshly sputter-deposited ITO films, exposed for just minutes to atmosphere, show that defect sites localized in the near-surface region are chemically reactive toward atmospheric water and hydrocarbons.[38] Typical ITO films (following solution and air- and oxygen-plasma etching) therefore show multiple forms of stoichiometric oxide and hydroxide and oxy-hydroxide forms in the near-surface region (shown schematically in Figures 2c and 2d). These indium hydroxide species appear to be weakly soluble in the presence of weak acids, and as shown below the electrochemical and electrical activity of these thin films can be impacted by simple small molecule chemisorption processes.

Small Molecule Chemisorption: Voltammetric Characterization of ITO with Adsorbed Small Molecules and Static Water Contact Angles after ITO Modification. Small molecules such as **1**, **2**, and **3** are readily chemisorbed to ITO surfaces, imparting both new electrochemical activity and lower surface polarity, without significant changes to surface roughness. Figure 3a shows the voltammetric characterization (in 0.25 M $LiClO_4$/acetonitrile) of two coverages of adsorbed **1** on ITO (adsorbed from a 10 mM ethanol solution for periods of 30 min and 6 h) versus the background voltammogram for a clean, unmodified ITO surface. The oxidation/reduction voltammetric peaks for adsorbed **1** are quite broad, owing to the heterogeneity in adsorption environments for **1** on these surfaces. Figure 3b shows the coulometrically determined coverage (mol/cm^2) of electroactive $Fc(COOH)_2$/ITO as a function of immersion time. The coverage of electroactive **1** rises at a moderate rate after initial immersion in the ethanol solution and reaches its maximum coverage (ca. 1×10^{-10} mol/cm^2) after ca. 200 min of solution adsorption. A compact monolayer of $Fc(COOH)_2$ can correspond to ca. $3-4 \times 10^{-10}$ mol/cm^2, based on molecule size (assuming both carboxylic acid groups are interacting with the surface, as assumed in Figure 2c) and a roughness factor of 1.1−1.2.[36,47−49,55] If we assume that only one carboxylic acid group interacts with the ITO surface (e.g., Figure 2d), then the anticipated coverage would of course be higher by as much as a factor of 2. The fact that the maximum electrochemically determined surface coverage is approximately one-third (or less) of the expected saturation monolayer coverage is most likely

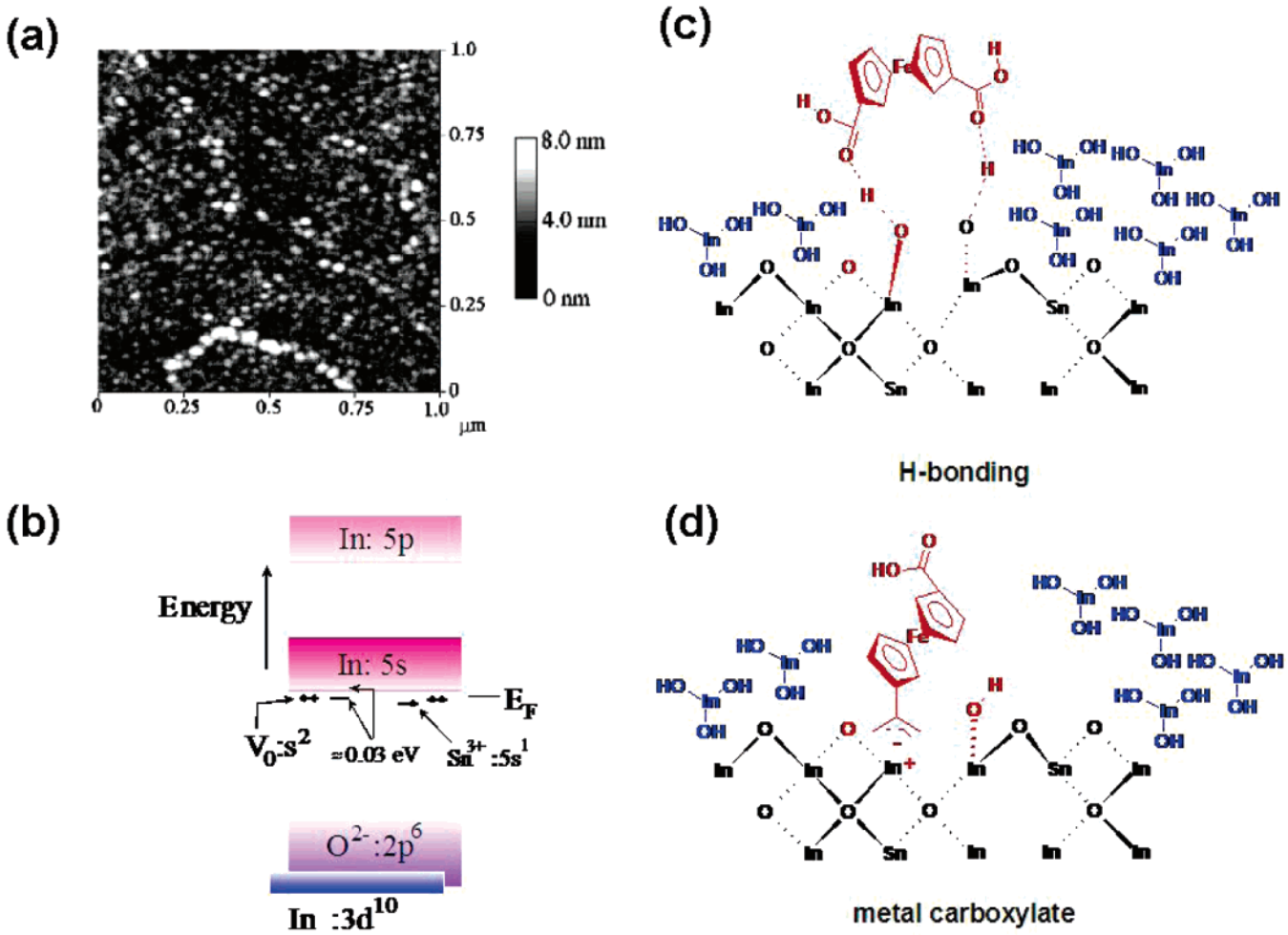

Figure 2. (a) Tapping mode AFM image of a typical cleaned ITO surface, either before or after chemisorption of the small molecules **1**−**3**. The rms surface roughness of these ITO samples was in the range of 1−3 nm before and after cleaning, plasma treatments, and small molecule chemisorption. (b) Proposed band structure for ITO films. The conductivity arises from both defects introduced into the ITO lattice during its sputter deposition and through the introduction of Sn^{3+} and Sn^{2+} ions, both of which can donate excess charge into the conduction band at room temperature (adapted from ref 54). (c and d) Schematic views of the proposed chemical states of the ITO surface, including adsorbed hydrolysis products and defect and dopant sites where the small molecule can adsorb either through electrostatic interactions, hydrogen bonding, and/or chelation of cation defect sites with carboxylates.[48−51]

due to the fact that only a fraction of the ITO surface is capable of supporting electron transfer to the adsorbed molecule; i.e., the total coverage of adsorbed **1** is significantly higher than the electroactive coverage. Conducting tip atomic force microscopy (AFM) studies of ITO electrodes by Scherer and co-workers[35] and our own recent studies[38] show that conventional ITO surfaces have widely varying electronic conductivities, with "electrically active" and "electrically inactive" regions distributed uniformly on submicron distance scales. Only after aggressive cleaning and pretreatment steps can 50−80% of the geometric area be rendered electroactive, and this state lasts in atmosphere for only a few minutes.[41]

Molecules **2** and **3** were chemisorbed in the same manner to ITO surfaces, for the same length of immersion time. The voltammetric characterization of adsorbed 3-TAA[51] shows a single irreversible voltammetric oxidation peak at ca. 1.0 V vs Fc/Fc^+, which was used to determine that its maximal electroactive surface coverage is well under a monolayer and close to that seen for **1**. Adsorbed **3** likewise showed voltammetric peak currents that increased with immersion time. The first one-electron oxidation of this molecule had an apparent $E°$ of ca. 0.3 V vs Fc/Fc^+; however, as with **1**, the voltammogram was quite broad, with the onset for oxidation occurring at ca. 0.1 V.[51] The onset for oxidation of the TPD core in **3** occurs at ca. 0.1 V negative of the $E°$ for the oxidation/reduction of solution TPD.[51,52] The coulometric analysis of the first one-electron oxidation/reduction peak for adsorbed **3** provided an estimate of its maximum surface coverage (ca. 5.0×10^{-11} mol/cm^2). AFM characterization of these small molecule modified ITO samples showed no appreciable difference in the rms roughness versus that shown in Figure 2a and no added topographic differences that might be attributed to aggregated materials adsorbed to the ITO surface. No changes in sheet resistance of these ITO samples were seen following modification with these small molecules.

Static water contact angles were measured for several ITO samples, exposed to each of the above modifiers, and the average contact angle from this series of measurements (ca. 20 measurements per modifier), following 8 h exposures to 0.01 M ethanol solutions of these small molecules, are shown in Table 1, compared with those of an ITO electrode modified with a thin film of PEDOT:PSS. As a control, we also show the contact angle for ITO samples exposed only to pure ethanol for the same length of time (8 h). Air- or oxygen-plasma-cleaned ITO samples are extremely polar, with water contact angles less than 5°. After exposure to ethanol these contact angles increase to ca. 31° and then nearly double again with chemisorption of

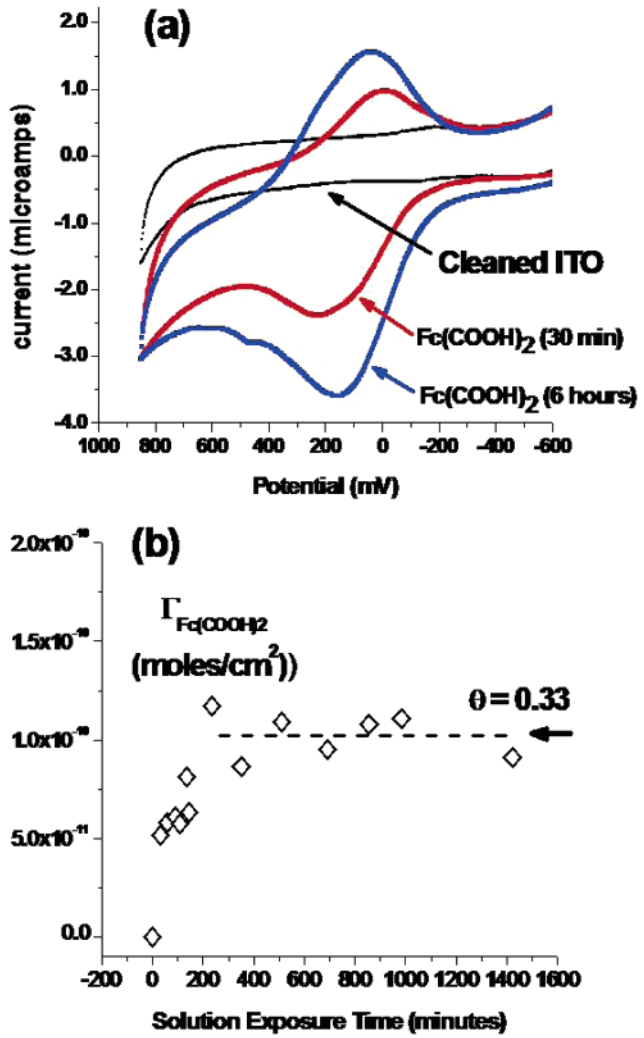

Figure 3. (a) Cyclic voltammograms of clean ITO and ITO with adsorbed **1**, in acetonitrile (0.1 M $LiClO_4$) for chemisorption times (from 10 mM $Fc(COOH)_2$/EtOH solutions) of 30 min and 6 h (0.1 V vs Fc/Fc^+). (b) Apparent standard electron-transfer rate coefficient ($k_{Fc/Fc^{+o}}$) for solution Fc/Fc^+ (1 mM in acetonitrile) vs surface coverage of **1**.

TABLE 1: Average Water Contact Angles for Unmodified and Modified ITO Electrodes and ITO Electrodes Overcoated with Either Spin-Cast Thin Films of PEDOT:PSS or Electrochemically Grown Films of PEDOT[a]

sample	average contact angle (deg)
air-plasma-etched ITO	<5
EtOH washed ITO	31.7
Piranha treated ITO	16.4
RCA cleaned	35.1
modified with **1**	51.2
modified with **2**	61.6
modified with **3**	55.2
spin-cast PEDOT:PSS (60 nm)	11.9
undoped PEDOT (electrochemically deposited)	29.5
doped PEDOT (electrochemically deposited)	39.5

[a] In aceotonitrile with 0.25 M $LiClO_4$.[51]

1, **2**, and **3** to ca. 51.2°, 61.4°, and 55.2°, respectively. It would be expected, however, that close-packed layers of these materials would lead to contact angles closer to 80−90°, suggesting that only a fraction of the polar hydroxide and oxy-hydroxide sites are associated with these small molecules. Interestingly, thin films of spin-cast PEDOT:PSS are more polar than both ethanol-soaked ITO surfaces and those modified with any of the above-mentioned small molecules.

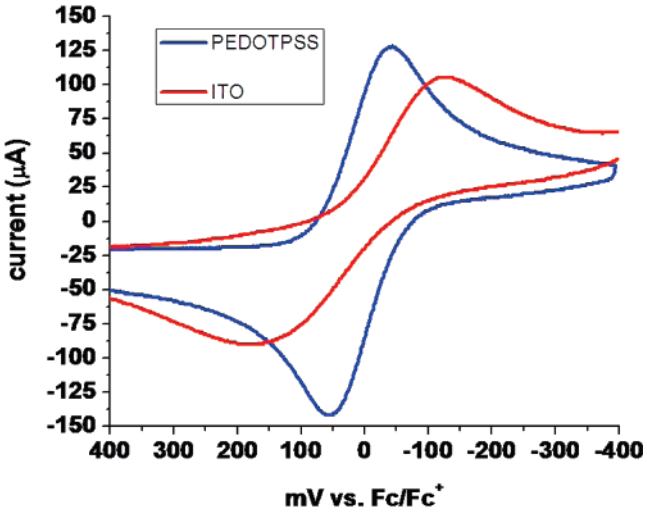

Figure 4. Voltammetric characterization of Fc/Fc^+ (0.01 V s^{-1} sweep rate) on bare ITO (air-plasma-etched after detergent/solvent cleaning) and bare ITO covered with a thin film of PEDOT:PSS (see text). For bare ITO the ΔE_p value of 0.37 V gave an estimated k_S value of 6.0×10^{-4} cm s^{-1}; for the PEDOT:PSS-modified ITO electrode $\Delta E_p = 0.096$ V and k_S = ca. 1.6×10^{-2} cm s^{-1}.

Electron Transfer to Solution Probe Molecules. Figure 4 shows the voltammetry of Fc/Fc^+ on bare, detergent/solvent-cleaned ITO and on an ITO electrode modified with a spin-cast PEDOT:PSS layer of a thickness of ca. 50 nm. The ITO electrodes used in these studies show broad anodic and cathodic peaks with large overpotentials for the Fc/Fc^+ redox couple, giving rise to a ΔE_p of ca. 365 mV at 0.01 V s^{-1} that corresponds to an effective rate coefficient for electron transfer, k_S, of ca. 6.0×10^{-4} cm s^{-1}. For clean Pt or Au electrodes in the same solvent the voltammetrically determined electron-transfer rate coefficient for Fc/Fc^+ is in the range of 1−4 cm s^{-1}.[56] We assume that the electroactivity of ITO is limited by the low surface coverage of accessible electroactive sites; i.e., these thin films can be modeled as partially blocked electrodes.[57−59] The fractional coverage of electroactive sites can be estimated from the relationship $k_S = k_S^\circ(1 - \theta)$,[57−61] where k_S° represents the electron-transfer rate (we assume a value of 1 cm s^{-1} [56]) coefficient determined for a totally unblocked electrode and $(1 - \theta)$ represents the fractional coverage of unblocked, electroactive sites. From the voltammetry for the clean ITO electrode in Figure 4 we estimate that the observed voltammetric response arises from ca. 1% or less of the geometric electrode area. Other sources of commercial ITO can provide higher rates of electron transfer and show a slightly higher fraction of electroactive surface area, and as shown below and in work to be reported soon from this group, chemical pretreatments can increase the electroactivity of these surfaces.[41] The thin PEDOT:PSS layer clearly mitigates some of these problems with ITO electroactivity; the k_S value has increased on the PEDOT:PSS-modified ITO surface to ca. 1.6×10^{-2} cm s^{-1}.

Figures 5 and 6 and Table 2 summarize the cyclic voltammetric oxidation/reduction behavior of the solution Fc and TPD on clean and ITO surfaces modified with **1**, **2**, and **3**. We chose acetonitrile as the solvent for these experiments, where the solution probes have high solubility and the chemisorbed modifiers **1**, **2**, and **3** are essentially insoluble. We also used

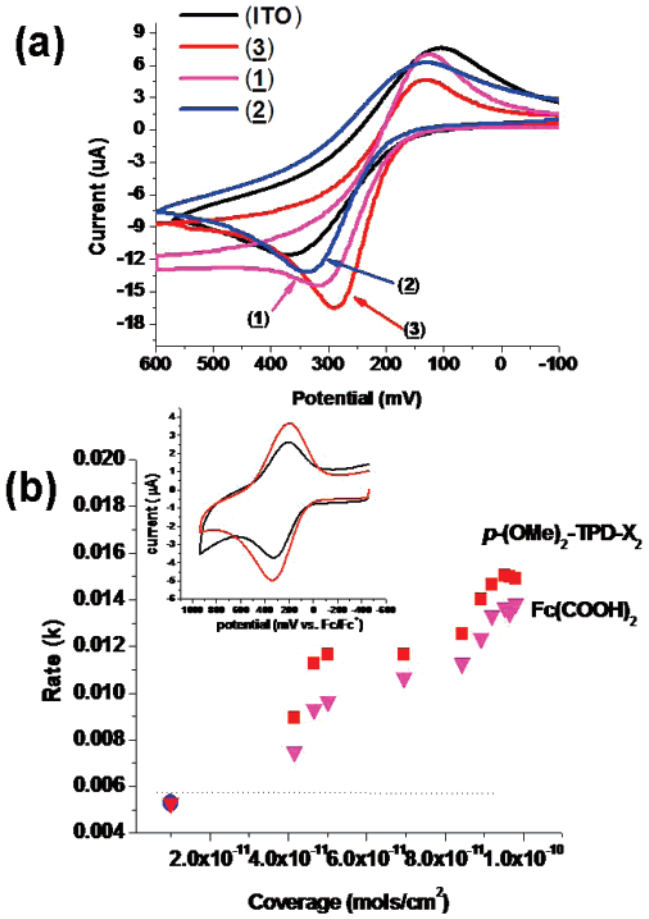

Figure 5. (a) Cyclic voltammograms of 1 mM Fc/Fc^+/MeCN (0.1 M $LiClO_4$) at clean ITO (black line) and ITO electrodes modified with small molecules **1**−**3** (see text) at their maximal coverages. (b) Apparent k^o_{Fc/Fc^+} vs surface coverage of **1** and **3**. The inset shows the voltammetry of adsorbed **1** at an as-cleaned and an air-plasma-etched ITO electrode, as in ref 34.

high supporting electrolyte concentrations (0.25 M $LiClO_4$) to minimize solution resistance effects on voltammetric peak separation.

Figure 5a shows the cyclic voltammetric behavior for Fc/Fc^+ on clean ITO and ITO electrodes modified with each small molecule, at sweep rates of 15 mV/second. For ITO electrodes modified with **1** and **3**, the peak current on the oxidative sweep was generally larger than that for the reduction sweep, suggestive of an electrocatalytic enhancement of the oxidation of Fc to Fc^+ at these low sweep rates.[62−64] The $E°$ for the oxidation/reduction of **1** is positive of that for Fc/Fc^+ by ca. 0.2 V; however, the 0.6 V peak width for the oxidation of surface-confined $Fc(COOH)_2$ means that ca. 80% of the electroactive adsorbed **1** has been oxidized at the $E°$ for oxidation of solution ferrocene; i.e., a substantial fraction of the surface-confined redox-active modifier can act to mediate charge transfer to solution Fc/Fc^+. The $E°$ value for surface-confined **3** is likewise positive of that for both solution Fc/Fc^+ and TPD/TPD^+, but because of the width of its voltammetric oxidation peak, at the anodic peak potential for the oxidation of solution Fc/Fc^+ we estimate that ca. 50% of surface-confined **3** has been converted to its oxidized form. As with surface-confined **1**, adsorbed monolayers of **3** have the potential to meditate electron transfer to a solution probe such as Fc/Fc^+.

The enhancement in peak current for the Fc/Fc^+ redox couple on electrodes modified with either **1** or **3** can arise from both an increase in the heterogeneous electron-transfer rate coefficient, k_S, arising from an "activation" of the ITO surface, and from an electrocatalytic effect, with rate coefficient k_{CAT}.[62−65] It is difficult to separate these two effects, since activation (slight etching) of the ITO surface may arise during long exposure periods to the carboxylic acid forms of these modifiers and the presence of adsorbed **1** or **3** near an electroactive site will mediate outer-sphere electron transfer to probe molecules such as Fc/Fc^+. The oxidation of **2**, however, occurs at potentials well positive of Fc/Fc^+, and some enhancement in oxidative peak current for Fc/Fc^+ still occurs after adsorption of **2**, which we conclude arises from an increase in the number of electroactive sites in the ITO surface.

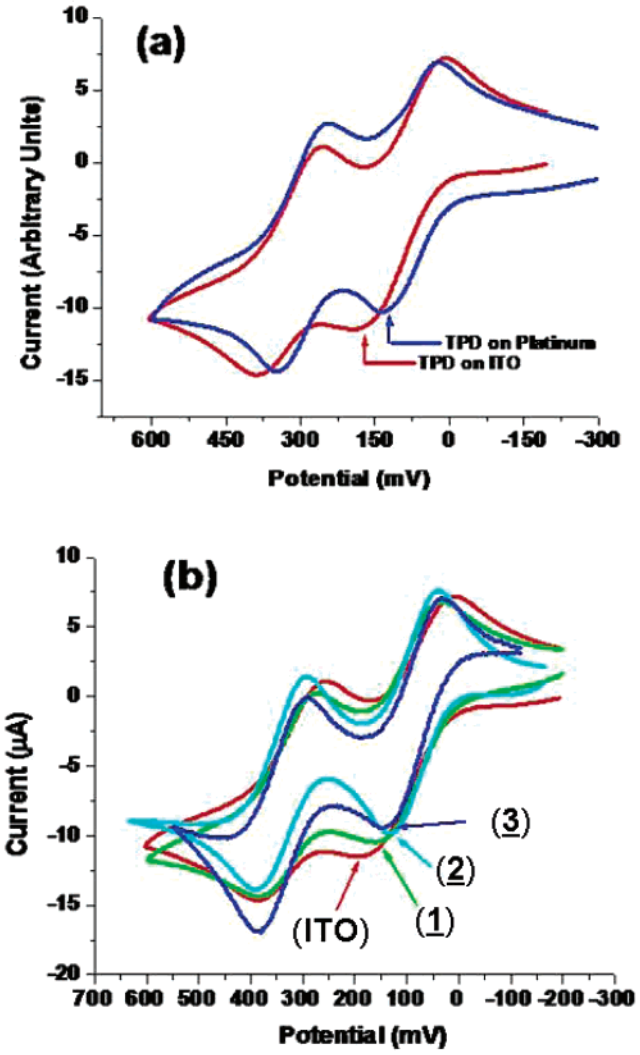

Figure 6. Cyclic voltammetric responses of 1 mM TPD in acetonitrile at (a) clean ITO and clean Pt electrodes and (b) ITO electrodes modified with chemisorbed **1**, **2**, and **3** at their maximal coverages (after chemisorption from 10 mM solutions in EtOH).

TABLE 2: Effective Electron-Transfer Rate Coefficients, k_S, Obtained at Clean Pt Electrodes, Unmodified ITO,[a] and ITO Electrodes Modified with Chemisorbed Monolayers of 1, 2, and 3

modification	k_S Fc/Fc^+	k_S TPD/TPD^+
Pt	0.7 cm s^{-1}	0.061 cm s^{-1}
unmodified ITO	0.6×10^{-3} cm s^{-1}	0.21×10^{-4} cm s^{-1}
1	3.9×10^{-3} cm s^{-1}	3.1×10^{-4} cm s^{-1}
2	3.3×10^{-3} cm s^{-1}	5.5×10^{-4} cm s^{-1}
3	5.3×10^{-3} cm s^{-1}	7.8×10^{-4} cm s^{-1}

[a] Detergent/solvent/air-plasma cleaned.

For TPD as a probe molecule we compared the voltammetric response on clean, unmodified ITO versus a clean Pt electrode (normalized for the same area) (Figure 6a) and after ITO modification with the same small molecule modifiers as discussed above (Figure 6b). Once again significant differences were seen for clean Pt versus clean ITO, with a lowering of the effective k_S value (first oxidation step) from 6.1×10^{-2} to 0.21×10^{-4} cm s^{-1}. We also compared the voltammetric response of ITO electrodes modified with the small molecule modifiers. Molecule **3** provided the largest increase in effective electron-transfer rates, showing an estimated increase to $k_S = 5.6 \times 10^{-4}$ cm s^{-1} for the first oxidation process, on the most optimized electrode surface.

These enhancements in voltammetric behavior were compared with those seen when a conducting polymer, such as PEDOT:PSS, was spin-cast onto the ITO surface, followed by voltammetry of Fc/Fc^+ in acetonitrile conducted in a similar manner to that discussed above. A ca. 50 nm layer of PEDOT:PSS provides a k_S value of 1.6×10^{-2} cm s^{-1}, which is larger than the enhancement seen on ITO surfaces modified with **1**, **2**, and **3**. As discussed below, however, enhancements in OLED device performance using the small molecule modifiers are nearly as large as those seen using PEDOT:PSS films alone, and using both the small molecule modifier (deposited first) and the PEDOT:PSS layer gives an even better OLED performance.

Surface Composition Changes as a Result of Small Molecule Chemisorption. It is interesting to note that the electroactive surface coverage for adsorbates **1**, **2**, and **3** is higher than would be predicted based on the percentage of electroactive sites determined from the solution voltammetry of Fc/Fc^+, where values of k_S indicate that electroactive sites on the unmodified surface constitute 1% or less of the geometric area. These results suggest that the chemisorption of small molecules not only provides a site for mediation of electron transfer but also changes the composition of the ITO surface to provide a higher fraction of electroactive sites.

XPS characterization of ITO surfaces following small molecule adsorption showed Fe(2p) bands consistent with $Fc(COOH)_2$ adsorption,[36,37,51] an increase in the higher binding energy O(1s) components (as expected from a slight increase in hydrolysis products and addition of oxygen in the adsorbed carboxylic acid groups), but no significant change to the In(3d) and Sn(3d) line shapes. UPS characterization of these surfaces showed only modest (less than 0.2 eV) decreases in the effective work function; thus the changes in device OLED performance shown below cannot be attributed to significant work function changes induced by the neutral molecules.

To further explore the surface compositional changes that result from small molecule chemisorption, high surface area In_2O_3 powders were exposed to the same solutions of **1**, **2**, or **3**, followed by IR characterization of the resultant powders in KBr pellets (Figure 7). The Fourier transform infrared (FTIR) spectra of these samples are compared with those of standard powders of $Fc(COOH)_2$ and a genuine sample of indium oxalate.[51] Neat $Fc(COOH)_2$ powder in KBr (Figure 7a) shows peaks at 1626 cm^{-1} ($\upsilon_{(C=O)}$) for the carboxylic acid functionality, 1480 cm^{-1} (C−O−H bend), 1410 cm^{-1} ($\upsilon_{(C-H)}$), and 1300 cm^{-1} ($\upsilon_{(C-O)}$), and these same peaks are seen for $Fc(COOH)_2$ adsorbed to the In_2O_3 powders. An additional peak at ca. 1550 cm^{-1} may be due to $\upsilon_{(C-O)}$ for a hydrogen-bonded form of $Fc(COOH)_2$.[65−67] Neat In_2O_3 powder, exposed to ethanol solution with no $Fc(COOH)_2$ for several hours, showed no new absorbance bands corresponding with the gain or loss of an adsorbed species (Figure 7b).

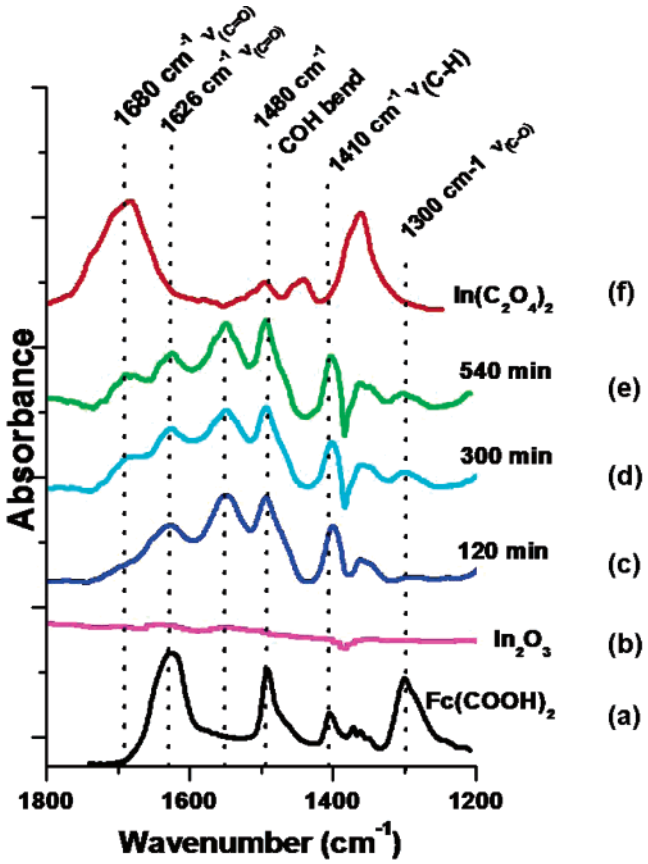

Figure 7. FTIR spectroscopic characterization of In_2O_3 powders as a function of immersion time in ethanol solutions with $Fc(COOH)_2$: (a) neat $Fc(COOH)_2$ powder/KBr pellet; (b) neat In_2O_3 powder, exposed to ethanol solution with no $Fc(COOH)_2$ for several hours, then dried and pressed into KBr; (c−e) In_2O_3 powder exposed to 10 mM $Fc(COOH)_2$/ethanol for 120, 300, and 540 min, dried and pressed into KBr pellets; (f) neat $In(C_2O_4)_2$ pressed into KBr. Peaks at 1626 cm^{-1} ($\upsilon_{(C=O)}$ for the carboxylic acid functionality), 1480 cm^{-1} (C−O−H bend), 1410 cm^{-1} ($\upsilon_{(C-H)}$), and 1300 cm^{-1} ($\upsilon_{(C-O)}$) are assigned to adsorbed $Fc(COOH)_2$. An additional peak at ca. 1550 cm^{-1} may be due to $\upsilon_{(C-O)}$ for a hydrogen-bonded form of $Fc(COOH)_2$.[65−67] The peak at ca. 1680 cm^{-1} ($\upsilon_{(C=O)}$—the easiest to unambiguously assign to an indium oxalate-like species) appears after the In_2O_3 powders have been exposed to the $Fc(COOH)_2$ solutions for times in excess of 2 h. The exposure time for first appearance of this band coincides with the increase in k_S for Fc/Fc^+ on ITO surfaces exposed to the same $Fc(COOH)_2$/ethanol solutions (Figures 3 and 4), suggesting that $Fc(COOH)_2$ is initially adsorbed via electrostatic and hydrogen-bonding interactions and at longer times with cation defect sites that can accommodate binding via coordination with the carboxylic acid groups in $Fc(COOH)_2$.[47,67,68]

For each chemisorption experiment approximately 500 mg of In_2O_3 powder was dispersed into an ethanol solution (e.g., 10 mM in $Fc(COOH)_2$) for periods of 0−540 min, following which FTIR characterization of the vacuum-dried powder was carried out. In_2O_3 powder exposed to 10 mM $Fc(COOH)_2$ in ethanol for 120, 300, and 540 min, dried and pressed into KBr pellets (Figure 7c−7e), showed many of the same peaks observed in Figure 7a associated with adsorbed $Fc(COOH)_2$. The peak at ca. 1680 cm^{-1} ($\upsilon_{(C=O)}$) is the most clearly assigned to an indium oxalate-like species,[65−67] appearing in both the $In(C_2O_4)_2$ standard powder/KBr (Figure 7f) and for In_2O_3 powders exposed to $Fc(COOH)_2$ solutions for times in excess of 2 h (Figures 7d and 7e). The exposure time for the first appearance of this band coincides with the increase in k_S for Fc/Fc^+ on ITO surfaces exposed to the same $Fc(COOH)_2$/ethanol solutions (Figures 3 and 4), suggesting that $Fc(COOH)_2$

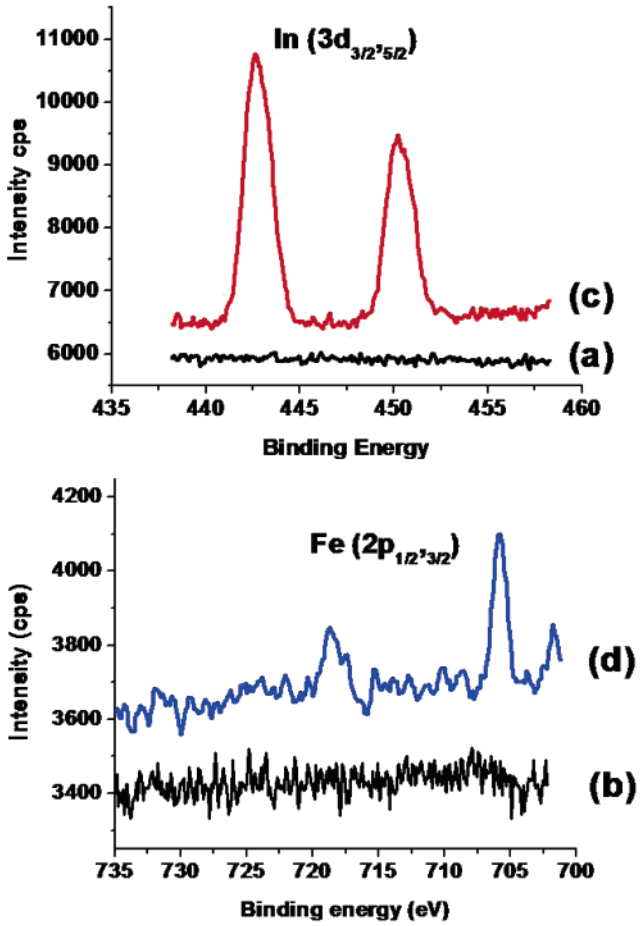

Figure 8. XPS spectra of the In(3d) and Fe(2p) regions for a Au surface, modified with a −COOH-terminated alkanethiol layer, before (a and b) and after (c and d) immersion into an EtOH solution with 0.01 M $Fc(COOH)_2$ and ca. 0.5 g In_2O_3 powder for ca. 8 h, followed by emmersion and rinsing. The growth of the In(3d) bands is consistent with some dissolution of free In^{3+} (or $In(OH)_3$) during the chemisorption of $Fc(COOH)_2$ to the In_2O_3 surface, which is subsequently chemisorbed to the −COOH groups terminating the alkanethiol monolayer. $Fc(COOH)_2$ is also bound to the −COOH-terminated alkanethiol surface (probably through hydrogen-bonding interactions), as indicated by the appearance of the Fe(2p) bands, which are at the same spectral position as those seen for $Fc(COOH)_2$ adsorbed to ITO surfaces.[2]

is initially adsorbed via electrostatic and hydrogen-bonding interactions and at longer times with cation defect sites that can accommodate binding via coordination with the carboxylic acid groups in $Fc(COOH)_2$.[65−67]

These surface compositional changes are quite subtle, requiring long immersion times, and suggest some dissolution of indium from the In_2O_3 or ITO surfaces brought about by chemisorption of $Fc(COOH)_2$ and related molecules. Our past XPS characterization of both materials has suggested that the powdered oxide is a reasonable high surface area "standard" for the ITO surface, showing comparable degrees of hydroxylation after exposure of the vacuum-dried powder to laboratory ambient environments.[36,55] Studies by inductively coupled plasma atomic emission spectroscopy of high surface area indium oxide powders exposed to small molecule carboxylate solutions suggest that trace levels of indium are liberated during the chemisorption event.[51] Additional confirmation of these compositional changes was sought by XPS analysis of a "capture surface" before and after exposure of these same In_2O_3 powders to small molecule modifiers such as $Fc(COOH)_2$ (Figure 8). In these experiments a 100 nm gold/glass thin film, with a full monolayer of a −COOH-terminated alkanethiol (HSC_{15}−COOH),[68] was left in a 10 mM $Fc(COOH)_2$/ethanol solution along with the In_2O_3 powder for periods of up to 8 h, following which the modified gold electrode was rinsed, dried, and characterized by XPS. In the absence of $Fc(COOH)_2$, these modified gold surfaces showed no uptake of either Fe or In, as seen in the Fe(2p) and In(3d) spectral regions (Figures 8a and 8b). With $Fc(COOH)_2$ in the solution the capture surface picked up appreciable amounts of both Fe and In, suggesting that (i) $Fc(COOH)_2$ itself will adsorb to the −COOH-terminated SAM (additional control experiments with no In_2O_3 powder were conducted to verify this), (ii) soluble In^{3+} ions are released from the In_2O_3 surface to be captured by the SAM−COOH surface through a combination of electrostatic and complexation events, and/or (iii) In^{3+} ions complexed by $Fc(COOH)_2$ are also captured by these −COOH-terminated surfaces. Options i and ii appear to us to be the most likely, and option ii is most significant for these studies. It is clear that there are slow chemical changes that can occur to the ITO surface as a result of long exposure to −COOH-bearing small molecules, which likely involve removal of some of the $In(OH)_x$-like surface species as soluble (complexed) indium. Although the layers removed from the ITO surface, followed by chemisorption of a less polar, electroactive molecule are probably quite thin (less than ca. 2−3 nm), these changes can have a profound effect on the wettability of the ITO surface, rates of charge injection, and as shown below the performance of simple organic diode devices. Other investigators have explored the instability of the ITO interface formed with PEDOT:PSS layers and have noted the release of free indium into OLEDs where the conducting polymer layer was applied just prior to device formation.[19] In our device studies our small molecule modified ITO samples were rinsed and dried prior to device formation; however we cannot discount the possibility that some free indium may still be available to migrate across the OLED during characterization.

Characterization of TPD/Alq_3 OLED Devices Utilizing Modified ITO Anodes. The same small molecule modification schemes were used on several similar sets of ITO substrates to test their effect on OLED performance (Figure 9). For these studies we chose simple vacuum-deposited TPD/Alq_3-based OLEDs,[53] which have sufficiently reproducible performance so that the effect of ITO modification could be clearly discerned. The device data shown in Figures 9a and 9b are from two different (carefully selected) sets of ITO samples, cut from the same general area of a larger sheet of commercially obtained ITO/glass. For most commercial sources of ITO there are sufficient variations in ITO composition and electrical properties across a 12 in. × 12 in. sheet of this material that one cannot simply randomly acquire the ITO samples for each set of devices. We carefully inspect each sheet of commercial ITO, using reflected light, to find regions that are similar in reflectivity and color, which has been found to ensure uniformity in the electrochemical performance for TCO films.[51] Generally, five OLED devices can be built on each 1 in. × 1 in. ITO substrate, and the variation in response from device to device is within acceptable limits (less than 0.15 V differences in onset bias, less than 0.07% differences in OLED device efficiencies). The variation in response between 4−5 1 in. × 1 in. ITO substrates is likewise less than the variations in response seen due to modification of the ITO substrates.

Figures 9a and 9b show the luminance (cd/m^2) and log(current) and device efficiency versus applied potential for a series of ITO/modifier/TPD/Alq_3/Mg:Ag OLEDs, where the ITO surface has been modified by exposure to 10 mM solutions of **1**, **2**, or **3** for periods of 8 h prior to device formation. For

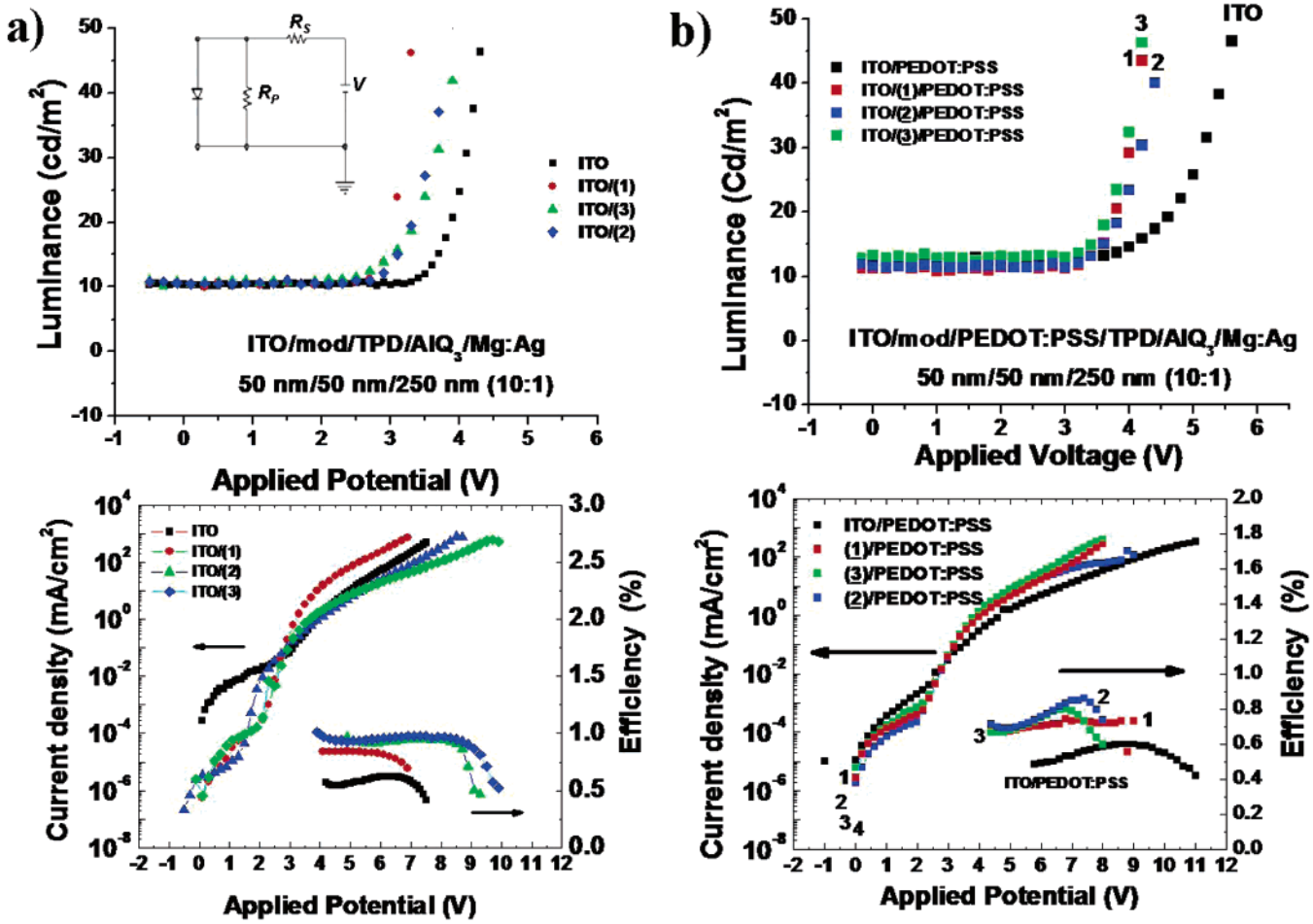

Figure 9. OLED device performance for OLEDs built on clean ITO and ITO modified with small molecules **1**, **2**, and **3**. The upper panels in parts a and b show luminance vs applied potential, while the lower panels show log current density and device power conversion efficiency vs applied potential. Plots in part a correspond to ITO/modifier/TPD/Alq_3/Mg:Ag devices, while plots in part b correspond to ITO/modifier/PEDOT:PSS/TPD/Alq_3/Mg:Ag devices. A simplified diode device schematic is shown in the inset of the upper panel in part a, showing both the series resistance, R_S, and the shunt resistance, R_P. Changes are seen in R_S after small molecule modification, but the predominant changes arise through increases in R_P, causing a significant lowering of leakage currents in these devices and hence an increase in device efficiency, whether or not a PEDOT:PSS layer is applied to the ITO substrate.

OLEDs without the intervening PEDOT:PSS layer the addition of any of the small molecule modifiers lowers the onset voltage for appearance of an electroluminescence response; the forward bias required to achieve ca. 50 cd/m^2 luminance (ca. 50% of average display brightness) is reduced by up to 2 V. Plotting the current−voltage behavior on a log scale makes clearer the contrast between the currents flowing at forward bias prior to electroluminescence (leakage currents) and those flowing during production of a visible electroluminescent response. At 1.0 V forward bias, the leakage current in these OLEDs drops from 5 $\times$ 10^{-6} A/cm^2 (clean ITO) to as low as 5 $\times$ 10^{-9} A/cm^2 after modification with **1**, **2**, or **3** (Figure 9a, lower panel), which is better than the reduction in leakage current achieved with addition of a spin-cast PEDOT:PSS layer to a clean ITO surface (Figure 9b, lower panel). We attribute this lowering of leakage currents primarily to a lowering of the pinhole density in the TPD layers in the OLED (increase in R_P), as a result of the lowered polarity brought about by small molecule chemisorption. The OLED device efficiency, measured at a forward bias of 5 V, nearly doubles when the small molecule modifiers are used (e.g., the efficiency for normally cleaned ITO is ca. 0.55%; the efficiency for an OLED modified with **1**, **2**, or **3** ranges from 0.8% to 1.0%, with **2** and **3** providing the greatest efficiency enhancement).

The upper and lower panels of Figure 9b show a series of OLED devices created using the spin-cast PEDOT:PSS layer alone and PEDOT:PSS layers applied after modification of the ITO surface with the same series of small molecule modifiers. The presence of the modifier lowered the leakage current by a factor of 10 versus the PEDOT:PSS treatment alone, lowered the onset voltage for electroluminescence, and increased the device efficiency by ca. 40−50%. It is clear that the presence of the small molecule as an intermediate between the bare ITO surface and the conducting polymer can play an important role in device operation.

It should also be noted that comparable changes in performance in single-layer OLEDs and "hole-only" organic diodes have been noted with this same set of small molecule modifiers.[51] In those experiments we created single-layer OLEDs based on polyvinylcarbazole (PVK) films into which we doped high concentrations of Alq_3 or its sulfonamide derivative, Al(qs)$_3$, to form devices with the configuration ITO/PVK:Alq_3/Al or just ITO/PVK/Al hole-only devices. In both device types chemisorption of the small molecule modifier lowered the onset voltage for current flow in the forward bias direction. In the case of the OLEDs, these small molecule modifiers also increased the overall OLED device efficiency. Fc(COOH)$_2$ and 3-TAA have also been evaluated as ITO modifiers in OPVs

based on vacuum-deposited phthalocyanine/C_{60}/bathocuproine (BCP) bilayer cells (ITO/CuPc/C60/BCP/Al), and there it was found that the presence of the modifier nearly doubled device power conversion efficiency.[37,38]

Conclusions

ITO modification through chemisorption of small molecule carboxylates (a) creates a less polar oxide surface, (b) slowly etches hydrolyzed indium oxide species from the near-surface region to enhance the fractional area that is truly electroactive, (c) enhances the rate of electron transfer to a solution probe molecule (if the modifier is electroactive in the same potential region as the surface modifier), and (d) significantly lowers the leakage currents, lowers the onset voltage for electroluminescence, and raises the overall efficiency in conventional vacuum-deposited OLEDs, whether a conductive polymer modifier layer such as PEDOT:PSS is used or not.

Other surface modification strategies for ITO and related TCO electrodes using chemisorption or covalent bonding of small molecules and polymers have been extensively studied to optimize the performance of OLED devices. Among the more successful of these strategies has been the formation of cross-linked siloxane polymer thin films on the ITO surface, which appear to improve OLED performance by providing a small barrier to hole injection, thereby balancing the arrival rates of holes and electrons at the organic heterojunction in the center of the OLED (e.g., the TPD/Alq_3 interface).[33,34] These modifications undoubtedly also promote wetting of the ITO/organic interface with hole transport layers by lowering the effective surface free energy of the ITO surface. The widespread use of spin-cast PEDOT:PSS and related conductive polymer dispersions also has a beneficial effect on OLED performance, due in part to the planarization of these substrates that can be achieved, the increase in the effective work function, and as shown in this paper the enhancements in charge injection rates that can arise from these conductive polymer layers.[19,42−45] If the sulfonic acid groups in these polymer dispersions are in the H^+ versus the Na^+ form, then there is a high probability that the effective pH at the ITO/PEDOT:PSS interface is low, promoting some of the etching behavior noted in this work using the small molecule carboxylate modifiers. It has been noted that the sodium content of the PEDOT:PSS film can significantly affect the electrical properties of ITO electrodes thus modified, but it is not yet clear whether this is associated with etching of the ITO surface.[45] The overall instability of the ITO/PEDOT:PSS interface continues to be of concern, and our studies here suggest that the ITO surface must be assumed to be a source of free indium whenever a moderately strong acid or chelating agent is used as the modifying agent.[36−38,41]

The work presented here confirms the efficacy of small molecule chemisorption as a route to TCO modification, creating a less polar surface, with enhanced electron-transfer rates to solution probe molecules but without the change in the effective work function of this surface associated with PEDOT:PSS treatments. Some of the enhancement in electron-transfer rates clearly can be attributed to the slow removal of hydrolyzed indium oxides from the near-surface region, apparently through formation of soluble metal carboxylates, which in subsequent papers will be shown to enhance the percentage of the ITO surface that is truly electroactive.[38,41] It is interesting that the adsorption of molecule **2**, which cannot mediate electron transfer to a solution probe molecule such as Fc/Fc^+, still promotes enhanced electron-transfer rates and enhanced OLED performance, which we hypothesize is due to the etching of the ITO surface and chemisorption of the small molecule modifier in freshly exposed metal cation defect sites.[41] The presence of free indium has been noted previously in both small molecule and polymer-based OLEDs, and it is clear that it may arise from a number of different processing protocols, including acid or base etchants and the use of PEDOT:PSS overlayers. It should be noted that recently reported work by Guo et al. also shows enhancements in performance in polymer-based OLEDs, where the PEDOT:PSS layer is replaced by a strongly chemisorbed phosphonic acid quaterthiophene monolayer that can be further doped to lower the barrier to hole injection.[29,32]

The electrochemical and device activation effects reported in this publication are most pronounced for ITO electrodes that have less than optimal electrochemical properties in their as-received state (detergent/solvent cleaning only). Conducting tip AFM studies of various forms of commercial ITO samples have recently shown a significant variation in electrical activity of as-received ITO samples, where the number density of electroactive sites in the near-surface region can range from ca. 10^6 per cm^2 up to 5×10^7 per cm^2, prior to any surface activation.[38,41] We have recently found that this variation can have a significant impact on both OLED and OPV device performance but that small molecule chemisorption still enhances both electrochemical performance and OLED and OPV device performance.

Work to be reported shortly focuses on the extrapolation of these studies to other modification protocols for ITO. The adsorption of carboxylic acid based small molecule modifiers can be used to initiate growth of "brushlike" conducting polymer thin films on ITO surfaces, which ultimately raises the voltammetrically determined value for k_S for solution ferrocene probe molecules to rival those seen for clean noble metal electrodes.[41] These modifications are preceded by very aggressive etching of the ITO surface with strong haloacids, removing up to 8 nm of the near-surface region prior to modification and greatly enhancing the electroactivity as seen both by electrochemical probes and by calibrated AFM.[38] Carboxylic acid and phosphonic acid small molecule modifiers in addition have been added to ITO substrates to provide for significant enhancements in OPV devices created by vacuum deposition of single organic/organic heterojunctions. Once again we can trace at least some of the improvement in device performance to near-surface etching and electrical activity improvements.

Acknowledgment. We gratefully acknowledge support for this research from the Office of Naval Research, the National Science Foundation (Grant Nos. CHE-0211900 and CHE-0517963), and the National Science Foundation Center for Materials and Devices for Information Technology (Grant No. DMR-0120967) (N.R.A.).

References and Notes

(1) Hartnagel, H. L.; Dawar, A. L.; Jain, A. K.; Jagadish, C. *Semiconducting Transparent Thin Films*; Institute of Physics Publishing: Bristol, U. K., 1995; pp 13−15, 175−187, 265−282.

(2) Forsythe, E. W.; Abkowitz, M. A.; Gao, Y. L.; Tang, C. W. *J. Vac. Sci. Technol., A* **2000**, *18*, 1869.

(3) Mason, M. G.; Hung, L. S.; Tang, C. W.; Lee, S. T.; Wong, K. W.; Wang, M. *J. Appl. Phys.* **1999**, *86*, 1688.

(4) Park, Y.; Choong, V.; Gao, Y.; Hsieh, B. R.; Tang, C. W. *Appl. Phys. Lett.* **1996**, *68*, 2699.

(5) Xue, J. G.; Forrest, S. R. *J. Appl. Phys.* **2004**, *95*, 1869.

(6) Malliaras, G. G.; Scott, J. C. *J. Appl. Phys.* **1998**, *83*, 5399.

(7) Shen, Y. L.; Jacobs, D. B.; Malliaras, G. G.; Koley, G.; Spencer, M. G.; Ioannidis, A. *Adv. Mater.* **2001**, *13*, 1234.

(8) Shen, Y. L.; Hosseini, A. R.; Wong, M. H.; Malliaras, G. G. *ChemPhysChem* **2004**, *5*, 16.

(9) Khodabakhsh, S.; Sanderson, B. M.; Nelson, J.; Jones, T. S. *Adv. Funct, Mater.* **2006**, *16*, 95.
(10) Veinot, J. G. C.; Marks, T. J. *Acc. Chem. Res.* **2005**, *38*, 632.
(11) Kim, J. S.; Cacialli, F.; Friend, R. *Thin Solid Films* **2003**, *445*, 358.
(12) Kim, J. S.; Friend, R. H.; Cacialli, F. *Appl. Phys. Lett.* **1999**, *74*, 3084−3086.
(13) Kim, J. S.; Friend, R. H.; Cacialli, F. *J. Appl. Phys.* **1999**, *86*, 2774.
(14) Kim, J. S.; Ho, P. K. H.; Thomas, D. S.; Friend, R. H.; Cacialli, F.; Bao, G. W.; Li, S. F. Y. *Chem. Phys. Lett.* **1999**, *315*, 307.
(15) Kim, J. S.; Granstrom, M.; Friend, R. H.; Johansson, N.; Salaneck, W. R.; Daik, R.; Feast, W. J.; Cacialli, F. *J. Appl. Phys.* **1998**, *84*, 6859.
(16) Ho, P. K. H.; Granstrom, M.; Friend, R. H.; Greenham, N. C. *Adv. Mater.* **1998**, *10*, 769.
(17) Sheats, J. R.; Roitman, D. B. *Synth. Met.* **1998**, *95*, 79−85.
(18) Sheats, J. R.; Chang, Y. L.; Roitman, D. B.; Stocking, A. *Acc. Chem. Res.* **1999**, *32*, 193.
(19) de Jong, M. P.; van Ijzendoorn, L. J.; de Voigt, M. J. A. *Appl. Phys. Lett.* **2000**, *77*, 2255.
(20) Taylor, D. M.; Morris, D.; Cambridge, J. A. *Appl. Phys. Lett.* **2004**, *85*, 5266.
(21) Nuesch, F.; Rothberg, L. J.; Forsythe, E. W.; Le, Q. T.; Gao, Y. *Appl. Phys. Lett.* **1999**, *74*, 880−882.
(22) Mason, M. G.; Hung, L. S.; Tang, C. W.; Lee, S. T.; Wong, K. W.; Wang, M. *J. Appl. Phys.* **1999**, *86*, 1688−1692.
(23) Warschkow, O.; Ellis, D. E.; Gonzalez, G. B.; Mason, T. O. *J. Am. Ceram. Soc.* **2003**, *86*, 1707.
(24) Warschkow, O.; Miljacic, L.; Ellis, D. E.; Gonzalez, G. B.; Mason, T. O. *J. Am. Ceram. Soc.* **2006**, *89*, 616.
(25) Popovich, N. D.; Wong, S. S.; Yen, B. K. H.; Yeom, H. Y.; Paine, D. C. *Anal. Chem.* **2002**, *74*, 3127.
(26) Popovich, N. D.; Wong, S. S.; Ufer, S.; Sakhrani, V.; Paine, D. *J. Electrochem. Soc.* **2003**, *150*, H255.
(27) Yaglioglu, B.; Huang, Y. J.; Yeom, H. Y.; Paine, D. C. *Thin Solid Films* **2006**, *496*, 89.
(28) Milliron, F. J.; Hill, I. G.; Shen, C.; Kahn, A.; Schwartz, J. *J. Appl. Phys.* **2000**, *87*, 572−576.
(29) Hanson, E. L.; Guo, J.; Koch, N.; Schwartz, J.; Bernasek, S. L. *J. Am. Chem. Soc.* **2005**, *127*, 10058.
(30) Span, A. R.; Bruner, E. L.; Bernasek, S. L.; Schwartz, J. *Langmuir* **2001**, *17*, 948.
(31) Milliron, D. J.; Hill, I. G.; Shen, C.; Kahn, A.; Schwartz, J. *J. Appl. Phys.* **2000**, *87*, 572.
(32) Guo, J.; Koch, N.; Bernasek, S. L.; Schwartz, J. *Chem. Phys. Lett.* **2006**, *426*, 370−373.
(33) Malinsky, J. E.; Veinot, J. G. C.; Jabbour, G. E.; Shaheen, S. E.; Anderson, J. D.; Lee, P.; Richter, A. G.; Burin, A. L.; Ratner, M. A.; Marks, T. J.; Armstrong, N. R.; Kippelen, B.; Dutta, P.; Peyghambarian, N. *Chem. Mater.* **2002**, *14*, 3054.
(34) Cui, J.; Wang, A.; Edleman, N. L.; Ni, J.; Lee, P.; Armstrong, N. R.; Marks, T. J. *Adv. Mater.* **2001**, *13*, 1476.
(35) Liau, Y. H.; Scherer, N. F.; Rhodes, K. *J. Phys. Chem. B* **2001**, *105*, 3282.
(36) Donley, C.; Dunphy, D.; Paine, D.; Carter, C.; Nebesny, K.; Lee, P.; Alloway, D.; Armstrong, N. R. *Langmuir* **2002**, *18*, 450−457.
(37) Armstrong, N. R.; Carter, C.; Donley, C.; Simmonds, A.; Lee, P.; Brumbach, M.; Kippelen, B.; Domercq, B.; Yoo, S. Y. *Thin Solid Films* **2003**, *445*, 342.
(38) Armstrong, N. R. Simmonds, A.; Veneman, A.; Schulmeyer, T.; Brumbach, M.; Xia, W.; Marikkar, F. S.; Singh, P. S.; Lee, P., to be submitted for publication.
(39) Doherty, W. J.; Wysocki, R. J.; Armstrong, N. R.; Saavedra, S. S. *J. Phys. Chem. B* **2006**, *110*, 4900−4907.
(40) Doherty, W. J.; Wysocki, R. J.; Armstrong, N. R.; Saavedra, S. S. *Macromolecules* **2006**, *39*, 4418−4424.
(41) Marrikar, F. S.; Brumbach, M.; Evans, D. H.; LeBron, A.; Wysocki, R.; Armstrong, N. R. *Langmuir*, submitted for publication.
(42) Cao, Y.; Yu, G.; Zhang, C.; Menon, R.; Heeger, A. J. *Synth. Met.* **1997**, *87*, 171−174.
(43) Greczynski, G.; Kugler, T.; Keil, M.; Osikowicz, W.; Fahlman, M.; Salaneck, W. R. *J. Electron Spectrosc. Relat. Phenom.* **2001**, *121*, 1.
(44) Kugler, T.; Salaneck, W. R. *C. R. Acad. Sci., Ser. IV: Phys., Astrophys.* **2000**, *1*, 409.
(45) de Kok, M. M.; Buechel, M.; Vulto, S. I. E.; van de Weijer, P.; Meulenkamp, E. A.; de Winter, S.; Mank, A. J. G.; Vorstenbosch, H. J. M.; Weijtens, C. H. L.; van Elsbergen, V. *Phys. Status Solidi A* **2004**, *201*, 1342.
(46) Nakao, T.; Nakada, T.; Nakayama, Y.; Miyatani, K.; Kimura, Y.; Saito, Y.; Kaito, C. *Thin Solid Films* **2000**, *370*, 155.
(47) Zotti, G.; Zecchin, S.; Vercelli, B.; Berlin, A.; Grimoldi, S.; Groenendaal, L.; Bertoncello, R.; Natali, M. *Chem. Mater.* **2005**, *17*, 3681.
(48) Vercelli, B.; Zotti, G.; Schiavon, G.; Zecchin, S.; Berlin, A. *Langmuir* **2003**, *19*, 9351.
(49) Zotti, G.; Schiavon, G.; Zecchin, S.; Berlin, A.; Pagani, G. *Langmuir* **1998**, *14*, 1728−1733.
(50) Gardner, T. J.; Frisbie, C. D.; Wrighton, M. S. *J. Am. Chem. Soc.* **1995**, *117*, 6927−6933.
(51) (a) Carter, C. Ph.D. Dissertation, University of Arizona, 2006. (b) Marrikar, F. S. Ph.D. Dissertation, University of Arizona, 2006.
(52) Anderson, J. D.; McDonald, E. M.; Lee, P. A.; Anderson, M. L.; Ritchie, E. L.; Hall, H. K.; Hopkins, T.; Mash, E. A.; Wang, J.; Padias, A.; Thayumanavan, S.; Barlow, S.; Marder, S. R.; Jabbour, G. E.; Shaheen, S.; Kippelen, B.; Peyghambarian, N.; Wightman, R. M.; Armstrong, N. R. *J. Am. Chem. Soc.* **1998**, *120*, 9646.
(53) Tang, C. W.; Vanslyke, S. A. *Appl. Phys. Lett.* **1987**, *51*, 913.
(54) Fan, J. C. C.; Goodenough, J. B. *J. Appl. Phys.* **1977**, *48*, 3524−3531.
(55) Donley, C. Ph.D. Dissertation, University of Arizona, 2003.
(56) Fawcett, W. R.; Opallo, M. *Angew. Chem., Int. Ed. Engl.* **1994**, *33*, 2131.
(57) Amatore, C.; Saveant, J. M.; Tessier, D. *J. Electroanal. Chem.* **1983**, *147*, 39−51.
(58) Amatore, C.; Saveant, J. M.; Tessier, D. *J. Electroanal. Chem.* **1983**, *146*, 37−45.
(59) Finklea, H. O.; Snider, D. A.; Fedyk, J.; Sabatani, E.; Gafni, Y.; Rubinstein, I. *Langmuir* **1993**, *9*, 3660−3667.
(60) Holt, K. B.; Bard, A. J.; Show, Y.; Swain, G. M. *J. Phys. Chem. B* **2004**, *108*, 15117−15127.
(61) Duo, I., Fujishima, A., Cominellis, C. H. *Electrochem. Commun.* **2003**, *5*, 695−700.
(62) Murray, R. W.; Ewing, A. G.; Durst, R. A. *Anal. Chem.* **1987**, *59*, A379 and references therein.
(63) Alleman, K. S.; Weber, K.; Creager, S. E. *J. Phys. Chem.* **1996**, *100*, 17050−17058.
(64) (a) Brookes, B. A.; Davies, T. J.; Fisher, A. C.; Evans R. G.; Wilkins, S. J.; Yunus, K.; Wilkins, S. J.; Wadhawan, J. D.; Compton, R. G. *J. Phys. Chem. B* **2003**, *107*, 1616−1627. (b) Davies, T. J.; Brookes, B. A.; Yunus, K.; Wilkins, S. J.; Greene, P. R.; Wadhawan, J. D.; Compton, R. G. *J. Phys. Chem. B* **2003**, *107*, 6431−6444.
(65) van den Brand, J.; Blajiev, O.; Beentjes, P. C. J.; Terryn, H.; de Wit, J. H. W. *Langmuir* **2004**, *20*, 6308−6317.
(66) Alexander, M. R.; Payan, S. *Surf. Interface Anal.* **1998**, *26* (13), 961−973.
(67) Hu, H.; Saniger, G.; Garciaalejandre, J.; Castano, V. M. *Mater. Lett.* **1991**, *12*, 281−285.
(68) Lee, T. R.; Carey, R. I.; Biebuyck, H. A.; Whitesides, G. M. *Langmuir* **1994**, *10*, 741−749.